# EUR 5286 e

COMMISSION OF THE EUROPEAN COMMUNITIES

# THE ANGULAR FLUX OF GAMMA RAYS IN A NORMAL CONCRETE SHIELD

by

H. PENKUHN

1974

Joint Nuclear Research Centre
Ispra Establishment - Italy

# LEGAL NOTICE



This report is on sale at the addresses listed on cover page 4

at the price of B.Fr. 90.—

**Commission of the European Communities**
**D.G. XIII - Directorate General for Scientific and Technical Information and Information Management**
29, rue Aldringen
Luxembourg
December 1974

**EUR 5286 e**

THE ANGULAR FLUX OF GAMMA RAYS IN A NORMAL CONCRETE SHIELD
by H. PENKUHN

Commission of the European Communities
Joint Nuclear Research Centre — Ispra Establishment (Italy)
Luxembourg, December 1974 — 18 Pages — 3 Figures — B.Fr. 90.—

The angular dependence of the photon energy and dose rate flux in an ordinary concrete slab shield is fitted near the shield axis by a power of the directional cosine $\omega = \cos \varphi$. The exponents found are strongly space-dependent. For large $\varphi$, further fits are given. The source energy range from 0.7 MeV to 6 MeV and penetrations of 12.5 cm $\leqq x \leqq$ 200 cm are considered.

**EUR 5286 e**

THE ANGULAR FLUX OF GAMMA RAYS IN A NORMAL CONCRETE SHIELD
by H. PENKUHN

Commission of the European Communities
Joint Nuclear Research Centre — Ispra Establishment (Italy)
Luxembourg, December 1974 — 18 Pages — 3 Figures — B.Fr. 90.—

The angular dependence of the photon energy and dose rate flux in an ordinary concrete slab shield is fitted near the shield axis by a power of the directional cosine $\omega = \cos \varphi$. The exponents found are strongly space-dependent. For large $\varphi$, further fits are given. The source energy range from 0.7 MeV to 6 MeV and penetrations of 12.5 cm $\leqq x \leqq$ 200 cm are considered.

**EUR 5286 e**

THE ANGULAR FLUX OF GAMMA RAYS IN A NORMAL CONCRETE SHIELD
by H. PENKUHN

Commission of the European Communities
Joint Nuclear Research Centre — Ispra Establishment (Italy)
Luxembourg, December 1974 — 18 Pages — 3 Figures — B.Fr. 90.—

The angular dependence of the photon energy and dose rate flux in an ordinary concrete slab shield is fitted near the shield axis by a power of the directional cosine $\omega = \cos \varphi$. The exponents found are strongly space-dependent. For large $\varphi$, further fits are given. The source energy range from 0.7 MeV to 6 MeV and penetrations of 12.5 cm $\leqq x \leqq$ 200 cm are considered.

CORRIGENDUM

**EUR 5286 e**

COMMISSION OF THE EUROPEAN COMMUNITIES

# THE ANGULAR FLUX OF GAMMA RAYS IN A NORMAL CONCRETE SHIELD

by

H. PENKUHN

1974

Joint Nuclear Research Centre
Ispra Establishment - Italy

E.S.I.S.

**EUR 5286 e**

COMMISSION OF THE EUROPEAN COMMUNITIES

# THE ANGULAR FLUX OF GAMMA RAYS IN A NORMAL CONCRETE SHIELD

by

H. PENKUHN

1974

**Joint Nuclear Research Centre**
**Ispra Establishment - Italy**

## ABSTRACT

The angular dependence of the photon energy and dose rate flux in an ordinary concrete slab shield is fitted near the shield axis by a power of the directional cosine $\omega = \cos \varphi$. The exponents found are strongly space-dependent. For large $\varphi$, further fits are given. The source energy range from 0.7 MeV to 6 MeV and penetrations of 12.5 cm $\leqq x \leqq$ 200 cm are considered.

# THE ANGULAR FLUX OF GAMMA RAYS IN A NORMAL CONCRETE SHIELD.

## Introduction

In gamma shielding problems, the spectra and their energy integrals (f.i. the buildup factors) are well known -at least in homogeneous geometries /1/. But little is published about the angular dependence of the scattered photons. As long as the shields were homogeneous slabs, this lack of knowledge was no problem. But if the shield contains bent ducts, the angular distribution also becomes interesting, since its knowledge at one bend allows realistic estimates of fluxes and doses at the next bend etc. (or at the detector).

## The Unscattered Angular Flux $\phi^{(o)}(x,\omega)$

We assume a plane monoenergetic surface source shielded by a slab with an attenuation coefficient $\mu_o$ at the source energy $E_o$. Then we have for positive $\omega$:

$$\phi^{(o)}(x,\omega) = A\,\omega^k \exp(-\mu_o x/\omega) = A\,\omega^k\left[\exp(-1/\omega)\right]^{\mu_o x}$$

$\omega = \cos\varphi$, $\varphi$ = ange between photon direction and shield axis
x = penetration along the axis
k = constant characterising the angular boundary flux
(f.i. $K = 0$ means isotropy, etc.)
A = normalisation constant

For small $\varphi$, we develop $1/\omega$ and the exponentials depending on $\varphi$ in power series in $\varphi$ and obtain:

$$\phi^{(o)}(x,\omega) \cong A\,\omega^k e^{-\mu_o x}\left[\exp\left(-\frac{\varphi^2}{2} - \frac{5\varphi^4}{24} - \frac{61\varphi^6}{720}\right)\right]^{\mu_o x}$$

$$\cong A\, e^{-\mu_o x}\,\omega^{k+\mu_o x} \exp\left(-\mu_o x\,\frac{\varphi^4}{8\omega}\right)$$

The error of the last approximation is of the order $\varphi^8/\omega^2$. Thus for a great range of x and $\omega$ (f.i. $\mu_o x \leq 20$ and $\varphi \leq 30°$) the angular dependence of $\phi^{(o)}(x,\omega)$ is given by the power $\omega^{k+\mu_o x}$. For thick shields and low $E_o$ this exponent can grow quite large (example: $E_o$= 0.7 MeV and x = 2 m in ordinary concrete mean $\mu_o x \approx 35$), so $\phi^{(o)}(x,\omega)$ gets extremely anisotropic. Thus a simple factorisation as "angular flux= spatial function times angular function" is impossible for the unscattered rays.

The Scattered Angular Flus

In order to get similar laws for the scattered intensity we apply our numerical gamma transport code PIPE /2/. We consider a concrete shield of 2.33 g/ccm, the ordinary concrete 01 in /3/*. A 1m thick slab source of the same material is assumed. Table 1 shows the results for $E_o$= 6 MeV. The first three columns give x in cm, x in mfp, then the energy build-up factor, and the following entries are $10^3 \times \phi_E^{(s)}(x,\omega) / \phi_E^{(s)}(x,1)$. The index $^{(s)}$ denotes the scattered energy fluxes, $\omega_i$ stands for the 9 used $\omega$-meshpoints. The last row gives the spatially averaged deviations of $D^{(s)}(x,\omega)/D^{(s)}(x,1)$ (D= dose or exposure rate) from $\phi_E^{(s)}(x,\omega)/\phi_E^{(s)}(x,1)$ in percents; 32$\pm$6 means differences ranging from 26 to 38%, $\phi_E$ is the energy flux .

*The dependence of the results on the sort of normal concrete is discussed in the annex.

# Table 1

$10^3 \left[\phi_E^{(s)}(x,\omega)/\phi_E^{(s)}(x,1)\right]$ for $E_0 = 6$ MeV

| x(cm) | $\mu_0 x$ | $B_E(x)$ | -1. | -.7 | -.3 | .0 | .3 | .6 | .8 | .9 | .97 |
|---|---|---|---|---|---|---|---|---|---|---|---|
| 12.5 | 0.787 | 1.73 | 18.6 | 23.9 | 41 | 84.7 | 374 | 728 | 891 | 951 | 985.5 |
| 25 | 1.574 | 2.02 | 12.5 | 15.7 | 25 | 44.6 | 149 | 488 | 760 | 886 | 966 |
| 50 | 3.15 | 2.55 | 7.6 | 9.5 | 14.5 | 23.3 | 55 | 239 | 544 | 766 | 926 |
| 100 | 6.30 | 3.60 | 4.5 | 5.6 | 8.3 | 12.6 | 25 | 92 | 322 | 589 | 857 |
| 150 | 9.45 | 4.63 | 3.3 | 4.1 | 6 | 9 | 17 | 53 | 210 | 468 | 880 |
| 200 | 12.6 | 5.67 | 2.7 | 3.3 | 4.9 | 7.2 | 13 | 38 | 150 | 325 | 749 |
| $D_{REL}^{(s)} - \phi_{E,REL}^{(s)}$ | | | | < $32 \pm 6$ > | | 31 $\pm 11$ | 21 $\pm 19$ | 14 $\pm 14$ | 5 $\pm 6$ | 2 $\pm 2$ | 0.5 $\pm 0.5$ |

The energy dependence of the conversion factor from energy flux to dose rate near 6 MeV (it rises with decreasing E) explains that $D^{(s)}(x,\omega)/D^{(s)}(x,1)$ is higher than $\phi_E^{(s)}(x,\omega)/\phi_E^{(s)}(x,1)$. Possible approximations are:

for $\varphi \leq$ arc cos 0.8 $\cong$ 37° $\cong$ 0.64 radian and 25 cm $\leq x \leq$ 200 cm

$$\phi_E^{(s)}(x,\omega)/\phi_E^{(s)}(x,1) \cong \omega^{n^{(s)}(x)} \quad \text{for } \omega \geqslant 0.8$$

with $n^{(s)}(x) = 0.87\left(\frac{x}{12.5\text{cm}} - 0.5\right)^{0.85} (1 \pm 10\%)$

for $\omega = 0$ (i.e. $\varphi = 90°$), 12,5cm $\leq x \leq$ 200cm, and

$\xi = x/(25\text{ cm})$

$$\phi_E^{(s)}(x,0)/\phi_E^{(s)}(x,1) = 0.0446 * \xi^{-0.888} (1 \pm 4\%)$$

for $\omega \leq 0$, 25cm $\leq x \leq$ 200 cm

$$\phi_E^{(s)}(x,\omega)/\phi_E^{(s)}(x,0) = (1-\omega)^{-1.65} (1 \pm 20\%)$$

for $0 \leq \omega \leq 0.8$, 25cm $\leq x \leq$ 200cm

$$\phi_E^{(s)}(x,\omega)/\phi_E^{(s)}(x,0) = \exp(3.6 * \omega)(1 \pm 20\%)$$

All deviations in % given here and afterwards are the occurring maxima, no averages. The function $n^{(s)}(x)$ can be defined not only as fitting parameter -as was done here- but also as averaged gradient with respect to $\omega$ of $\phi_E^{(s)}(x,\omega)/\phi_E^{(s)}(x,1)$ near $\omega = 1$:

$$n^{(s)}(x) = \frac{\partial}{\partial\omega}\left[\phi_E^{(s)}(x,\omega)/\phi_E^{(s)}(x,1)\right]_{\omega \approx 1}$$

All these values relative to $\phi_E^{(s)}(x,1)$ or $\phi_E^{(s)}(x,0)$ can be normalised by means of the buildup factor:

$$\left[B_E(x)-1\right] * \phi_E^{(o)}(x) = \iint_{4\pi} \phi_E^{(s)}(x,\omega)\, d\Omega = 2\pi \int_{-1}^{1} \phi_E^{(s)}(x,\omega)\, d\omega$$

($d\Omega$ = element of solid angle). We must write $B_E(x)-1$ in the square brackets, since $B_E(x)$ refers to the total energy flux $\phi_E(x,\omega)$ - not only to the scattered one. In table 1,

$B_E(x)$ is listed for a t=1m thick concrete slab source; this means:

$$\phi_E^{(p)}(x) = \frac{E_0 Sv}{2\mu_0}\left[E_2(\mu_0 x)-E_2(\mu_0 x+\mu_0 t)\right]\approx\frac{E_0 Sv}{2\mu_0}E_2(\mu_0 x)$$

Sv = volume source strength in source slab, in phot/ccm/sec

$E_2(y)$= second exponential integral = $y\int_y^{\infty}(e^{-t}/t^2)dt$

The second term in the square brackets was ignored since $\mu_0 t = 6.3$ means

$$E_2(\mu_0 x+\mu_0 t)\leq e^{-6.3}\,E_2(\mu_0 x)\approx E_2(\mu_0 x)/545$$

Similar calculations for the source energy $E_0$= 3 MeV (source and shield geometry unchanged) yield the results of Table 2. Again the ratios $D^{(s)}(x,\omega)/D^{(s)}(x,1)$ are higher than their $\phi_E^{(s)}$-equivalents; but the difference decreases if $E_0$ decreases. This should be due to the slower change with energy of the conversion factor from energy flux to dose rate at 3 MeV than at 6 MeV. A comparison of tables 1 and 2 shows that a lower $E_0$ means lower anisotropy. The physical reason is that the compton scattering process described by the Klein-Nishina - formula (/4/ p. 140) becomes for low source energies less anisotropic. Possible approximations of the results in table 2 are:

$$\phi_E^{(s)}(x,\omega)/\phi_E^{(s)}(x,1)\approx\omega^{n^{(s)}(x)}\quad\text{for }\omega\geq 0.8$$

with $n^{(s)}(x) = 1.32\left(\frac{x}{12.5\text{cm}} - 0.5\right)^{0.7}(1\pm21\%)$

$$\phi_E^{(s)}(x,0)/\phi_E^{(s)}(x,1) = 0.0638\,\xi^{-0.722}(1\pm4\%)$$

with $\xi$= x/(25cm). For $\omega\leq 0$ and $\xi\geq1$ we have

$$\phi_E^{(s)}(x,\omega)/\phi_E^{(s)}(x,0)=(1-\omega)^{-1.57}(1\pm19\%)$$

## Table 2

$$10^3 \left[ \phi_E^{(s)}(x,\omega)/\phi_E^{(s)}(x,1) \right] \text{ for } E_o = 3 \text{ MeV vs. } x \text{ and } \omega$$

| x(cm) | $\mu_o x$ | $B_E(x)$ | $\omega_i$: −1.0 | −.7 | −.3 | .0 | .3 | .6 | .8 | .9 | .97 |
|---|---|---|---|---|---|---|---|---|---|---|---|
| 12.5 | 1.06 | 2.41 | 31.8 | 40.1 | 63.5 | 110. | 320. | 651. | 843. | 926. | 977.4 |
| 25 | 2.12 | 3.05 | 21.6 | 26.9 | 40.4 | 63.8 | 142. | 412. | 694. | 846. | 952. |
| 50 | 4.25 | 4.32 | 13.9 | 17.2 | 25.1 | 37.7 | 71. | 207 | 491. | 715. | 905. |
| 100 | 8.5 | 6.95 | 9.0 | 11.0 | 15.8 | 22.9 | 40. | 100. | 292. | 543. | 831. |
| 150 | 12.75 | 9.69 | 7.0 | 8.6 | 12.3 | 17.9 | 30. | 71. | 206. | 436. | 773. |
| 200 | 17 | 12.55 | 5.9 | 7.3 | 10.3 | 14.8 | 25. | 58. | 162. | 363. | 723. |
| $D^{(s)}_{REL} - \phi^{(s)}_{E,REL}$ (%) | | | 10 ±4 | 12 ±3 | 15 ±4 | 16 ±6 | 13 ±10 | 11 ±10 | 5.5 ±5.5 | 2.4 ±2.4 | 0.8 ±0.8 |

and for $0 \leq \omega \leq 0.6$

$$\phi_E^{(s)}(x,\omega)/\phi_E^{(s)}(x,0) = \exp(2.8*\omega)(1 \pm 28\%)$$

Similar calculations for $E_o$ = 1.25 MeV yield table 3. The anisotropy at $E_o$=1.25 MeV is still lower than at $E_o$ = 3 MeV. The fact that the differences

$$\frac{D^{(s)}(x,\omega)}{D^{(s)}(x,1)} - \frac{\phi_E^{(s)}(x,\omega)}{\phi_E^{(s)}(x,1)}$$

become negative for $E_o$ = 1.25 MeV (while they were positive for $E_o$ = 3 MeV and $E_o$ = 6 MeV) can be explained by the fact that the conversion factor from energy fluence to dose is a flat function of energy at E $\lesssim$ 1 MeV and then shows a minimum at $E \approx 100$ KeV. Possible approximations of the data in table 3 are:

$$\phi_E^{(s)}(x,\omega)/\phi_E^{(s)}(x,1) = \omega^{n^{(s)}(x)}$$

for $0.9 \leq \omega \leq 1$ and with

$$n^{(s)}(x) = 1.65\left(\frac{x}{12.5\text{ cm}} - 0.5\right)^{0.68} (1 \pm 21\%)$$

for $\omega \leq 0$

$$\phi_E^{(s)}(x,\omega)/\phi_E^{(s)}(x,0) = (1-\omega)^{-1.3} (1 \pm 9\%)$$

for $0 \leq \omega \leq 0.8$

$$\phi_E^{(s)}(x,\omega)/\phi_E^{(s)}(x,0) = \exp(2.23*\omega) (1 \pm 23\%)$$

and finally, with $\xi = x/(25\text{ cm})$

$$\phi_E^{(s)}(x,0)/\phi_E^{(s)}(x,1) = 0.099\ \xi^{-0.433}(1 \pm 10\%)$$

As a last case, we take $E_o$= 0.7 MeV and obtain table 4.

# Table 3

$E_o = 1.25\text{MeV};\ 10^3 \left[\phi_E^{(s)}(x,\omega)/\phi_E^{(s)}(x,1)\right]$ VS. $\omega$ and x

| x(cm) | $\mu_o x$ | $B_E(x)$ | < | | | | $\omega_1$ | | | | > |
|---|---|---|---|---|---|---|---|---|---|---|---|
| | | | −1 | −.7 | −.3 | 0.0 | 0.3 | 0.6 | 0.8 | 0.9 | 0.97 |
| 12.5 | 1.66 | 4.51 | 56 | 68 | 100 | 148 | 290 | 567 | 783 | 891 | 966 |
| 25 | 3.31 | 6.83 | 40 | 49 | 69 | 99 | 166 | 360 | 624 | 797 | 933 |
| 50 | 6.62 | 12.3 | 29 | 35 | 49 | 69 | 109 | 220 | 448 | 668 | 883 |
| 100 | 13.2 | 25.6 | 22 | 27 | 37 | 51 | 79 | 153 | 312 | 525 | 812 |
| 150 | 19.9 | 42.0 | 19 | 23 | 32 | 44 | 68 | 130 | 259 | 449 | 761 |
| 200 | 26.5 | 61.1 | 17.6 | 21 | 29 | 40 | 62 | 117 | 232 | 401 | 719 |
| $D_{REL}^{(s)} - \phi_{E,REL}^{(s)}$ (%) | | | −18 $\pm 2$ | −15 $\pm 3$ | −11 $\pm 3$ | −7 $\pm 2$ | −3 $\pm 2$ | < | −1 $\pm 1$ | | > |

## Table 4

$$10^3 \left[ \phi_E^{(s)}(x,\omega)/\phi_E^{(s)}(x,1) \right] \text{ vs. } x \text{ and } \omega, \quad E_0 = 0.7 \text{ MeV}$$

| x(cm) | $\mu_0 x$ | $B_E(x)$ | < | | | | $\omega_i$ | | | | > |
|---|---|---|---|---|---|---|---|---|---|---|---|
| | | | -1. | -.7 | -.3 | .0 | .3 | .6 | .8 | .9 | .97 |
| 12.5 | 2.19 | 7.59 | 74 | 88 | 123 | 173 | 290 | 533 | 752 | 872 | 959 |
| 25 | 4.38 | 13.6 | 56 | 66 | 90 | 124 | 190 | 355 | 599 | 777 | 942.5 |
| 50 | 8.76 | 30.1 | 44 | 52 | 70 | 95 | 142 | 253 | 453 | 659 | 876 |
| 100 | 17.5 | 81.1 | 37 | 43 | 58 | 79 | 117 | 205 | 359 | 550 | 816 |
| 150 | 26.3 | 157 | 35 | 40 | 54 | 73 | 108 | 188 | 326 | 501 | 777 |
| 200 | 35.1 | 257 | 33 | 39 | 52 | 70 | 103 | 179 | 310 | 473 | 747 |
| $D_{REL}^{(s)} - \phi_{E,REL}^{(s)}$ (%) | | | -14 ± 1 | -11 ± 3 | -10 ± 2 | - 8 ± 2 | - 5 ± 3 | - 3 ± 2 | - 2 ± 2 | - 1 ± 1 | -.2 ±.2 |

The negative signs in the last row are explained similarly as for $E_0 = 1.25$ MeV. Possible approximations are :

for $0.9 \leq \omega \leq 1$

$$\phi_E^{(s)}(x,\omega)/\phi_E^{(s)}(x,1) = \omega^{n^{(s)}(x)}$$

with $n^{(s)}(x) = 1.48\sqrt{\mu_0 x - 1.3}\ (1 \pm 20\%)$

$$\phi_E^{(s)}(x,0)/\phi_E^{(s)}(x,1) = 0.127\ \xi^{-0.332}\ (1 \pm 8\%)$$

for $-1 \leq \omega \leq 0.6$ (!)

$$\phi_E^{(s)}(x,\omega)/\phi_E^{(s)}(x,0) = (1-\omega)^{-1.14}\quad (1 \pm 12\%)$$

for $0 \leq \omega \leq 0.6$

$$\phi_E^{(s)}(x,\omega)/\phi_E^{(s)}(x,0) = \exp\ (1.8 * \omega)\ (1 \pm 16\%)$$

and for $-1 \leq \omega \leq 0.9$ even

$$\phi_E^{(s)}(x,\omega)/\phi_E^{(s)}(x,0) = 1/(1-\omega)\ \left[1 \pm 23\%\right]$$

It should be noted that even the worst errors of all our approximations, $\pm 28\%$, are still in the order of magnitude of the errors to be expected for such differential data as the directional energy flux in deep-penetration problems. (Such integral data as the build-up factors are known with better precision).

The different degree of anisotropy for different $E_0$

Fig. 1 shows the curves $n^{(s)}$ and $n^{(o)}$ vs $\mu_0 x$ and $E_0$. $n^{(o)}$ is independent on $E_0$ and strictly linear in $\mu_0 x$; $n^{(s)}$ changes with $E_0$ and $\mu_0 x$, and at constant $\mu_0 x$ a lower $E_0$ means a lower $n^{(s)}$, i.e. more isotropy. If we plot our other fitting parameters vs. $E_0$, we obtain the same result: lower $E_0$ means less anisotropy; but even at 0.7 MeV source energy we are far from isotropy: at x=100 cm (or $\mu_0 x = 17.5$) $\phi_E^{(s)}(x,\omega)$ changes by a factor 27 between $\omega = -1$ and $\omega = 1$.

Our other fitting parameters are f.i. the exponent of $1-\omega$, that of $\xi$, the coefficient before the $\xi$-power, and the coefficient before $\omega$ in the argument of the exponential.

Comparison with other works

There are few results comparable to ours since most work on angular spectra was done either for backscattering or for skyshine, /5/ ch.4. But recent calculations of W.Zumach /8/ with the DOT code confirm our result of the strong dependence of $n^{(s)}$ upon x. Early calculations of Trubey /6/, /7/ p. 123 - 127, resulted in a nearly space-independent $n^{(s)}(\mu_o x)$; but they cover only the range $1.5 \leq \mu_o x \leq 4.5$ for $E_o$=0.662 MeV in Al for a collimated source. This means an unscattered angular spectrum of the same shape (delta-function!) everywhere, thus also the scattered angular spectrum has a nearly space-independent shape. But our isotropic source leads to a strong dependence of $\phi_E^{(o)}(x,\omega)$ on $\omega$ in the shield - and therefore of $\phi_E^{(s)}(x,\omega)$, too.

But we can compare our values with those of Raso and the NRDL experiments /7/, /9/. We divide the NRDL values by $\omega = \cos \varphi$ (they refer to a current, ours to a flux detector) and multiply ours by $\sin\varphi$ ; our data are per steradian (unit solid angle $d\Omega$), but NRDL is per radian, i.e. per unit angle $d\varphi$ . Since $d\Omega = 2\pi \sin\varphi\, d\varphi$ , the conversion factor is $\sin\varphi$ , if an unimportant constant factor is ignored. Fig. 2 gives the comparison of the normalised curves for $E_o$= 1.25 MeV, fig. 3 for $E_o$ = 0.662 resp. 0.7 MeV. The deviations remain in the range $\pm$12% for $E_o$= 1.25 MeV and at $\mu_o x$ = 4.38 for $E_o$= 0.7 MeV; they reach $\pm$20% for $E_o$= 0.7 MeV at $\mu_o x$= 2.19. The deviations can be due to the experiments or the calculational approximations; at $\mu_o x$=2.19 and $E_o$= 0.7 MeV there can also be boundary effects, and the slight difference between $E_o$= 0.7 MeV and $E_o$=0.662MeV can produce a higher degree of isotropy at lower $E_o$.

In any case the differences lie within the range expected for differential results.

A further comparison of our buildup factors with those of the moments method /1/, /4/ for Al (after applying to them a correction for our volumic source and interpolating them) leads to an averaged difference of 7% for $E_0$= 3 MeV (maximum 11%), and for $E_0$=0.7 MeV an average of 14% (maximum 26%). The fact that nearly all our results were below those of /1/ , and that the deviations for $E_0$= 0.7 MeV increase systematically with penetration could be explained by the hypothesis that -especially at low source energies - the differences between aluminum and concrete become noticeable.

## Annex

### A Sensitivity Test

The considered concrete 01 contains much Ca (0.581 g/ccm). Is it really representative for other normal concretes? Therefore some calculations were done for the normal concrete 04 /3/ with only 0.194 g Ca/ccm. For $E_0$= 0.7 MeV the energy flux ratios were higher than those in table 4 by at most 1.5% for $\omega \geq 0.8$, by 0 to 5% for $0 \leq \omega \leq 0.6$, and by 3 to 9% for $\omega \leq -0.3$. For $E_0$= 3 MeV the deviations were $< 1\%$ for $\omega \geq 0.8$, 0 to 3% for $0 \leq \omega \leq 0.6$, and 2 to 6% for $\omega \leq -0.3$. Thus differences between the angular spectra in different normal concretes are negligible, especially near the shield axis where $\omega \sim 1$ and $\varphi < 1$.

## Acknowledgement

The author thanks his colleagues U.Canali (CCR Ispra), W.Futtermenger and Prof. H.Schultz (T.U. Hannover) for their discussions and proposals and moreover Miss M.R.Zocchi for typing the manuscript.


## References


/1/ H.Goldstein, J.E.Wilkins Jr., Calculation of the Penetration of Gamma Rays, NYO 3075, June 1954.

/2/ H.Penkuhn, How to use the Gamma Transport Code PIPE, EUR 4624 e; User's Manual for the Gamma Transport Codes BIGGI 3P and BIGGI 4T, EUR 3555e.

/3/ ANL 5800, Reactor Physics Constants, 2nd ed. (1963), p.660 (p.476 in 1st ed.).

/4/ H.Goldstein, Fundamental Aspects of Reactor Shielding, Addison-Wesley, Reading, Mass, 1959.

/5/ R.G.Jaeger (ed.), Engineering Compendium on Radiation Shielding, Vol.I, Springer Verlag.

/6/ USAEC report ORNL 2389, p. 220.

/7/ E.Blizzard, L.Abbott, Reactor Handbook Vol. III, Part B (Shielding).

/8/ W.Zumach, Augsburg, private communication.

/9/ D.J.Raso, Transmission of Scattered Gamma Rays through Concrete and Iron Slabs, Report TO-B 59-13; Technical Operations Inc., 1959, quoted in /7/ p. 125.

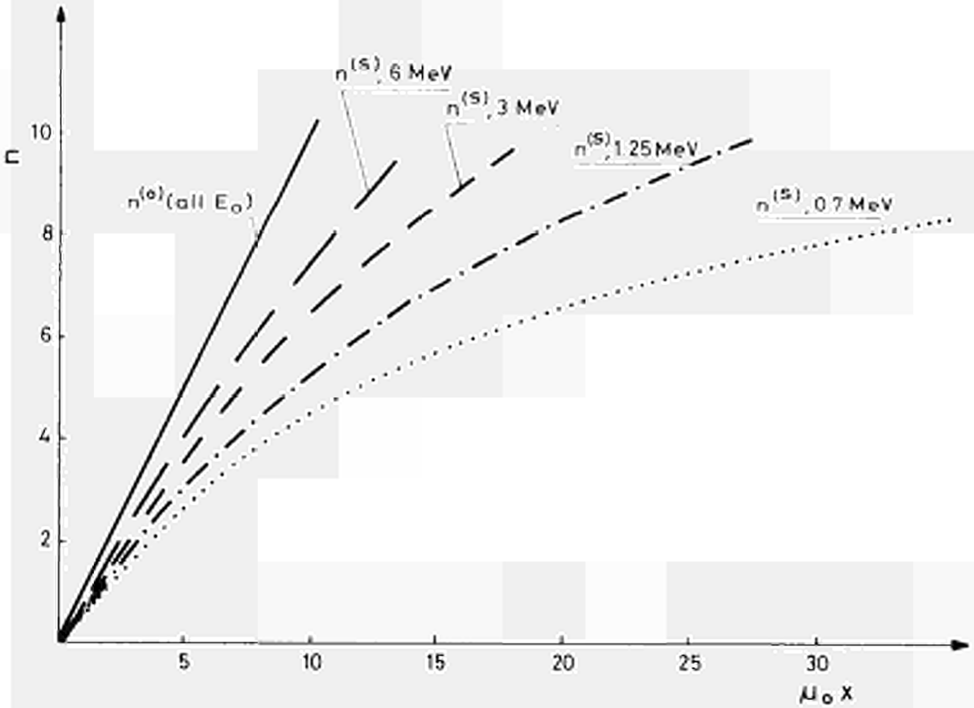


Fig. 1 : DIRECTIONAL EXPONENTS $n^{(o)}$ OF UNSCATTERED AND $n^{(S)}$ OF SCATTERED RAYS ( VALID FOR ANGULAR COSINES $\omega \gtrsim 0.85$ ) VS. PENETRATION $\mu_o x$ AND SOURCE ENERGY $E_o$

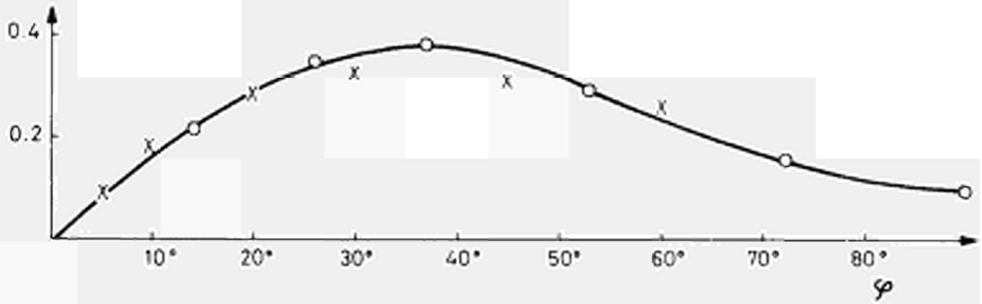


Fig. 2 : ANGULAR SPECTRUM FOR $E_o$ = 1.25 MeV. CURVE : THIS WORK, AT $\mu_o x$ = 3.31 IN CONCRETE. CROSSES : NRDL EXPERIMENT AT $\mu_o x$ = 3.40 IN AL (NORMALISED)

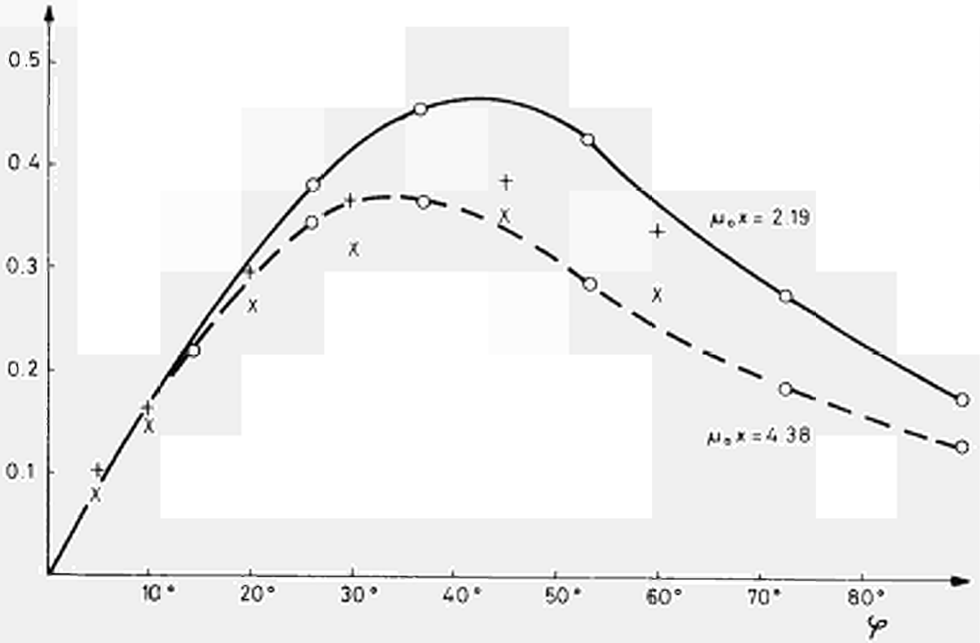


Fig. 3 : ANGULAR SPECTRA. CURVES : THIS WORK $E_o$ = 0.7 MeV. IN CONCRETE, $\mu_o x$ = 2.19, AND $\mu_o x$ = 4.38. CROSSES + : NRDL, AL, $\mu_o x$ = 2.05 ; CROSSES X : NRDL, AL, $\mu_o x$ = 4.11. FOR NRDL $E_o$ = 0.662 MeV.

## NOTICE TO THE READER

All scientific and technical reports published by the Commission of the European Communities are announced in the monthly periodical **"euro-abstracts"**. For subscription (1 year : B.Fr. 1 025,—) or free specimen copies please write to :

**Office for Official Publications**
**of the European Communities**
**Case postale 1003**
**Luxembourg 1**
**(Grand-Duchy of Luxembourg)**

To disseminate knowledge is to disseminate prosperity — I mean general prosperity and not individual riches — and with prosperity disappears the greater part of the evil which is our heritage from darker times.

Alfred Nobel

# SALES OFFICES

**The Office for Official Publications sells all documents published by the Commission of the European Communities at the addresses listed below, at the price given on cover. When ordering, specify clearly the exact reference and the title of the document.**

UNITED KINGDOM

*H.M. Stationery Office*
P.O. Box 569
London S.E. 1 — Tel. 01-928 69 77, ext. 365

BELGIUM

*Moniteur belge — Belgisch Staatsblad*
Rue de Louvain 40-42 — Leuvenseweg 40-42
1000 Bruxelles — 1000 Brussel — Tel. 512 00 26
CCP 50-80 — Postgiro 50-80

*Agency :*
Librairie européenne — Europese Boekhandel
Rue de la Loi 244 — Wetstraat 244
1040 Bruxelles — 1040 Brussel

DENMARK

*J.H. Schultz — Boghandel*
Møntergade 19
DK 1116 København K — Tel. 14 11 95

FRANCE

*Service de vente en France des publications des Communautés européennes — Journal officiel*
26, rue Desaix — 75 732 Paris - Cédex 15ᵉ
Tel. (1) 306 51 00 — CCP Paris 23-96

GERMANY (FR)

*Verlag Bundesanzeiger*
5 Köln 1 — Postfach 108 006
Tel. (0221) 21 03 48
Telex: Anzeiger Bonn 08 882 595
Postscheckkonto 834 00 Köln

GRAND DUCHY OF LUXEMBOURG

*Office for Official Publications of the European Communities*
Case postale 1003 — Luxembourg
Tel. 4 79 41 — CCP 191-90
Compte courant bancaire: BIL 8-109/6003/200

IRELAND

*Stationery Office — The Controller*
Beggar's Bush
Dublin 4 — Tel. 6 54 01

ITALY

*Libreria dello Stato*
Piazza G. Verdi 10
00198 Roma — Tel. (6) 85 08
CCP 1/2640

NETHERLANDS

*Staatsdrukkerij- en uitgeverijbedrijf*
Christoffel Plantijnstraat
's-Gravenhage — Tel. (070) 81 45 11
Postgiro 42 53 00

UNITED STATES OF AMERICA

*European Community Information Service*
2100 M Street, N.W.
Suite 707
Washington, D.C., 20 037 — Tel. 296 51 31

SWITZERLAND

*Librairie Payot*
6, rue Grenus
1211 Genève — Tel. 31 89 50
CCP 12-236 Genève

SWEDEN

*Librairie C.E. Fritze*
2, Fredsgatan
Stockholm 16
Post Giro 193, Bank Giro 73/4015

SPAIN

*Libreria Mundi-Prensa*
Castello 37
Madrid 1 — Tel. 275 51 31

OTHER COUNTRIES

*Office for Official Publications of the European Communities*
Case postale 1003 — Luxembourg
Tel. 4 79 41 — CCP 191-90
Compte courant bancaire: BIL 8-109/6003/200

OFFICE FOR OFFICIAL PUBLICATIONS OF THE EUROPEAN COMMUNITIES
Case postale 1003 — Luxembourg 6761

CDNA05286ENC